01 Jan 2007

Optimal Wide Area Controller and State Predictor for a Power System

Salman Mohagheghi

Ganesh K. Venayagamoorthy
Missouri University of Science and Technology

Ronald G. Harley

Recommended Citation

S. Mohagheghi et al., "Optimal Wide Area Controller and State Predictor for a Power System," *IEEE Transactions on Power Systems*, Institute of Electrical and Electronics Engineers (IEEE), Jan 2007.
The definitive version is available at https://doi.org/10.1109/TPWRS.2007.895158

Optimal Wide Area Controller and State Predictor for a Power System

Salman Mohagheghi, *Student Member, IEEE*, Ganesh K. Venayagamoorthy, *Senior Member, IEEE*, and Ronald G. Harley, *Fellow, IEEE*

***Abstract*—An optimal wide area controller is designed in this paper for a 12-bus power system together with a Static Compensator (STATCOM). The controller provides auxiliary reference signals for the automatic voltage regulators (AVR) of the generators as well as the line voltage controller of the STATCOM in such a way that it improves the damping of the rotor speed deviations of the synchronous machines. Adaptive critic designs theory is used to implement the controller and enable it to provide nonlinear optimal control over the infinite horizon time of the problem and at different operating conditions of the power system. Simulation results are provided to indicate that the proposed wide area controller improves the damping of the rotor speed deviations of the generators during large scale disturbances. Moreover, a robust radial basis function network based identifier is presented in this paper to predict the states of a multimachine power system in real-time. This wide area state predictor (WASP) compensates for transport lags associated with the present communication technology for wide area monitoring of the electric power grid. The WASP is also robust to partial loss of information caused by larger than expected transport lags or even failed sensors throughout the network.**

***Index Terms*—Adaptive critic designs, missing sensor restoration algorithm, multimachine power system, neural networks, radial basis functions, state estimation, transport lag, wide area control.**

I. Introduction

THE electric power grid in general consists of components such as synchronous generators, transmission lines, transformers, loads, active/reactive compensators, switches and relays. The compensators are shunt or series elements such as capacitors and inductors or power electronic converter based flexible ac transmission system (FACTS) devices.

Typically, the voltages at the terminals of the synchronous generators are controlled by automatic voltage regulators (AVR) in order to maintain a proper voltage profile throughout the network. Until now, designs of the internal controllers of a generator (voltage regulator and governor) have traditionally considered only the single generator and ignored other controlled devices in the power network. Extra stabilizing capabilities are sometimes provided for certain generators by utilizing power system stabilizers (PSS), which are mostly designed to increase the damping of the local low frequency oscillation mode of the generator [1]. Similarly, designers of FACTS device controllers consider only the FACTS device and ignore neighboring generator controllers for example [2].

In such a decentralized control structure, each internal/local controller acts as an *agent* to maximize a local performance index without any information about the overall system objectives. Based on their own information, these agents make control decisions in order to comply with the desired behavior of the decentralized system [3]. Therefore, all these internal control schemes, whether for the synchronous generator or the FACTS device, focus on controlling each component from an internal point of view. However, with a number of these controlled devices close to one another in a power network, the issue of interaction between them arises, that at times can lead to adverse effects causing inappropriate control effort by different agents. This happens since each agent attempts to be a good local controller, but has no information about the overall control objective of the entire system.

An alternative solution to the above issues can be a *multilevel control technique*, also referred to as a *multi-agent hierarchical control structure*, a supervisory level control or wide area control (WAC). The objective here is to define a set of sub-problems that can be considered independent at a certain level (subsystem level). Different from both centralized and decentralized control, a multi-agent control structure employs a number of semi-autonomous agents that collaborate with each other to achieve a given task [4]. Such a regime requires communication and coordination not among all the agents, but only among those closely related agents with common interests [5]. Although the agents communicate with one another, each agent performs primarily based on its own interest; therefore care should be taken that no agent's actions should violate its own limits.

It is normally assumed that the WAC coordinates the actions of the various agents throughout the network by using the supervisory control and data acquisition (SCADA) system, phasor measurement units (PMU) or other wide area dynamic information systems [6]. The WAC would receive data from the power system and, based on the defined objective functions, would send appropriate control signals to the agents in the power network, in order to optimize the overall system performance. However, even with the best communication channels there can be transport lags in sending/receiving the data across the network that are nonnegligible. The more entities using a communication channel, the slower the flow of information will

Manuscript received September 6, 2006; revised December 19, 2006. This work was supported by the National Science Foundation under Grants ECS 0400657 and ECS 0348221 and by the Duke Power Company, Charlotte, NC. Paper no. TPWRS-00591-2006.

R. G. Harley and S. Mohagheghi are with the Intelligent Power Infrastructure Consortium (IPIC), School of Electrical and Computer Engineering, Georgia Institute of Technology, Atlanta, GA 30332-0250 USA (e-mail: rharley@ece.gatech.edu; salman@ece.gatech.edu).

G. K. Venayagamoorthy is with the Real-Time Power and Intelligent Systems Laboratory, Department of Electrical and Computer Engineering, University of Missouri, Rolla, MO 65409-0249 USA (e-mail: gkumar@ieee.org).

Color versions of one or more of the figures in this paper are available online at http://ieeexplore.ieee.org.

Digital Object Identifier 10.1109/TPWRS.2007.895158

be. Any wide area control scheme has to be able to compensate for these transport lags.

This paper proposes neural network based structures for wide area control and state prediction of a 12-bus power system together with a STATCOM. The proposed controller provides simultaneous auxiliary control signals for the synchronous generators and the STATCOM in the power system and thereby improves the damping of the system during large scale disturbances. The advantages of the proposed WAC and the wide area state predictor (WASP) are as follows.

- WAC is designed based on a model-free approach, in which no mathematical model of the power system and no prior information on its parameters is necessary.
- WAC is able to provide optimal control over the infinite horizon of the problem in the presence of noise and uncertainties.
- Proposed WASP is able to compensate for static and dynamic transport lag associated with the communication channels across the power system.
- More importantly, using the available healthy data, the proposed WASP is able to restore missing information due to failed sensors or longer than usual delays. This helps keep the hierarchical controller in the control loop even when the required information is temporarily not available.

A survey of the previous work done on the supervisory level control in power systems is presented in Section II. The structure of the multimachine power system with the STATCOM appears in Section III. Section IV provides an overview of the suggested structure for the wide area state predictor. The structure and training scheme of the neural network based WAC is presented in Section V of the paper. Typical simulation results appear in Section VI in order to illustrate the effectiveness of the proposed WASP and WAC. Section VII summarizes some technical issues on implementing the WAC. Finally, the conclusions are given in Section VIII.

II. Previous Work on Wide Area Control in Power Systems

Several ideas have been proposed in the literature for controlling a power system from a supervisory level. Arafeh [7] published one of the first papers on the concepts of the hierarchical control theory in power systems. He designed a heuristics based hierarchical controller to enable the real-time control of a large scale power distribution system in terms of security (equipment protection) and operation (continuity of service). Rubaai and Villaseca [8] proposed an optimal hierarchical controller for improving the transient stability of a multimachine power system. The control technique involved a number of independent local controllers that communicate with a central coordinating controller. A similar approach was used by Okou *et al.* [9] to design a two level hierarchical controller using remote signals in order to improve power system stability under severe contingencies. Also, Posser *et al.* [10] applied the methodology of discrete-event systems (DES) and supervisory control to the transmission line restoration problem, in order to increase the steady state security level of a power network during restoration. Recently, Taylor *et al.* [11] proposed a wide area control system for discontinuous control of a power system in the form of sending signals for tripping the synchronous generators and/or switching reactive power sources.

In addition, much of the work in the past few years has focused on designing a global PSS. Aboul-Ela *et al.* [12] designed a PSS that uses global signals in addition to the local control signals and can be used for damping inter-area oscillations as well as the ones caused by the local modes. Chow *et al.* [13] also incorporated a second input to the PSS from one of the neighboring generators, as an auxiliary control signal for the PSS controller. Kamwa *et al.* [14] applied a similar technique by incorporating additional remote signals to a selected number of PSSs in the Hydro-Quebec's transmission system. Also, Ni *et al.* [4] designed a robust fuzzy logic based supervisory level PSS by using wide area measurements.

It has also been shown that with the introduction of auxiliary signals, FACTS devices can contribute to the dynamic and/or transient stability of the power system [2]. This issue has been investigated by some researchers in an attempt to design supervisory level controllers for different FACTS devices [5], [12], [13]. Also, Chaudhuri *et al.* [15] have designed an H_∞ based optimal supervisory level controller for a Static Var Compensator (SVC) in order to improve the damping of inter-area oscillations. The controller proposed in [15] showed a robust performance considering signal transmission delay of up to 0.75 s.

The complexity of a large power network often makes it very difficult for an analytically based control technique to perform a supervisory level control of the system. This is partly due to the fact that classical control schemes depend on a mathematical model of the plant to be controlled, and this model is often derived based on linearizing the power system at a specific operating condition. Moreover, as the control scheme moves from an external controller to a wide area scheme coordinating several local controllers, the complexity of the multi-input multi-output system is exponentially increased. This makes the design of the classical controller more tedious and at some instances impractical. Artificial intelligent techniques on the other hand, have the capability of dealing with such a nonlinear, nonstationary system in the presence of noise and uncertainties. Neural networks, for example, have been used to design an optimal wide area stabilizer for providing extra damping for the generator rotor speeds [16]. Also, Kim and Lee [17] presented an artificial neural network based coordination control scheme for an under load tap changing (ULTC) transformer and a STATCOM in order to minimize both the amount of tap changes of the transformer and STATCOM output while maintaining an acceptable voltage magnitude at the substation bus. Taylor *et al.*. [18] designed a fuzzy based wide area stability and control system, which provided rapid implementation of generator tripping and reactive power compensation switching for transient stability and voltage support of a power system.

III. 12-Bus Test Power System With a Static Compensator

In order to illustrate the neural network based wide area controller, the 12-bus test system in Fig. 1 is used. It contains three generators and has been proposed to evaluate the effects of FACTS devices in the transmission level [19]. Preliminary simulation results in [20] showed that installing a STATCOM

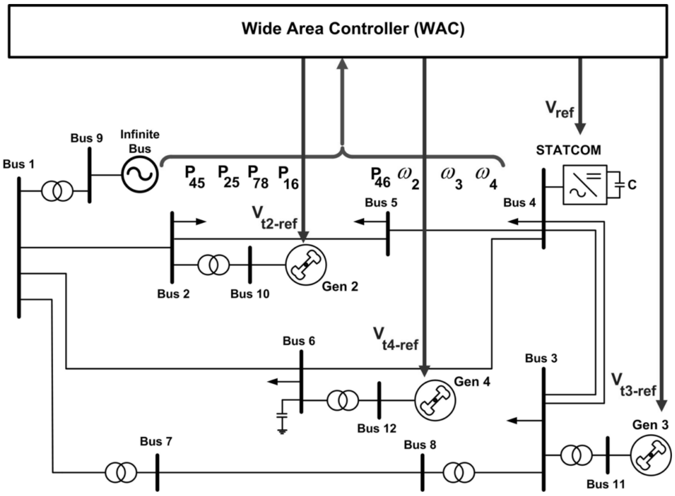

Fig. 1. Schematic diagram of the 12-bus test power system with a STATCOM.

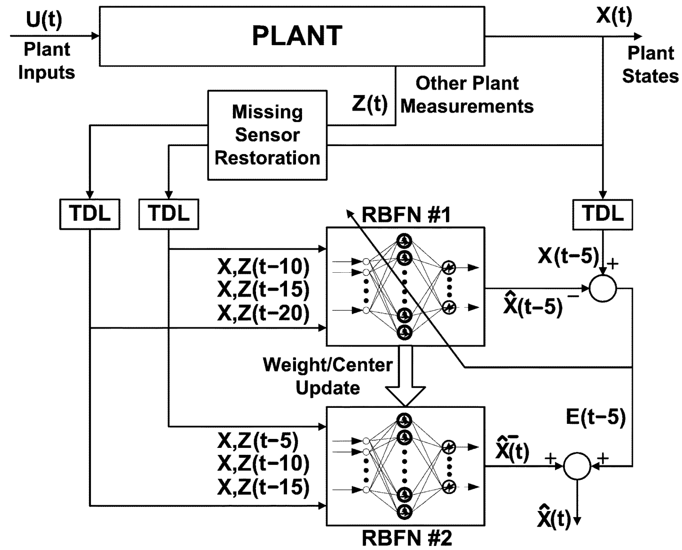

Fig. 2. Schematic diagram of the wide area state predictor.

at bus 4 can drastically improve the voltage profile of the whole network. The main control objective of the STATCOM in this study is to control the voltage at the point of common coupling (PCC) during both small and large scale disturbances.

The WAC receives the system states/measurements from across this power system, analyzes the data and sends the appropriate auxiliary signals to the voltage references of the three generators' AVRs $(V_{\mathrm{t2-ref}}, V_{\mathrm{t3-ref}}, V_{\mathrm{t4-ref}})$ and to the STATCOM line voltage controller (V_{ref}). The control objective of the WAC in this study is to improve the dynamic stability of the power system and increase the damping of the rotor speed deviations of the three generators during large scale disturbances. Since the global measurements throughout the network will reach the WAC with a transport lag, a WASP is used to compensate for the delay. The structure of the WASP is explained in the next section.

IV. Wide Area State Predictor (WASP)

A. Conventional State Estimation: Challenges and Limitations

The WAC is highly dependent on the accuracy and timing of the data received, which emphasizes the need for a reliable wide area state predictor capable of estimating the states of the system in real-time. Any system/technique designed for such a purpose should address the following issues.

- There is a transport lag associated with the communication channels used in power networks. The average communication delay could be as long as seconds for the internet or as short as tens of milliseconds in a fiber optic link [21]. The retrieval of real-time information from the received delayed values should be possible.
- The transport lag is not necessarily static. In the worst case, it can be a missing sensor or a failed communication channel. The methodology should be robust to the partial loss of information and should be able to restore the required data using the available information.
- Any changes to the power network configuration can largely deteriorate the effectiveness of the state estimator. Care should be taken that the estimator adaptively adjusts itself to the ever changing nature of the power network.

Numerical analysis methods are traditionally employed in order to solve the state estimation problem in power systems. However, as the dimension of the power system increases, the complexity level of the solution rises. This can specifically be a problem when a large number of redundant measurements are used in a power network. Moreover, the estimator functions/equations need to be adaptively adjusted as the power system operating conditions and configurations change. Clearly, incorporating the updates into the mathematical formulation of the state estimation problem can be a tedious process. Dependence on the model of the process is the major disadvantage of this technique, which can weaken its robustness and practicality in real world problems. In addition, the analytical state estimation method converges slowly, can become trapped in local minima or produce ill-conditioned and unreliable solutions [22]. Ideally, state estimation should run at the scanning rate; however, due to computational limitations most practical estimators run every few minutes or whenever a major change occurs [23].

B. Radial Basis Function Network Based WASP

Fig. 2 illustrates the schematic diagram of the proposed WASP. It consists of two major components: the radial basis function network (RBFN) and the missing sensor restoration (MSR) algorithm. The former uses the time delayed values for predicting the states of the power system in real-time, while the latter ensures that the RBFN has access to the best estimates of its input vector in case of loss of information and/or failed sensors.

1) WASP Structure and Development: The core of the proposed WASP consists of two radial basis function networks (RBFN) that together predict the power system states in real-time. The values of the plant state vector X and the measurement vector Z at time steps $(t - \Delta t)$, $(t - 2 \cdot \Delta t)$, $(t - 3 \cdot \Delta t)$ and $(t - 4 \cdot \Delta t)$ are used in order to predict the plant states at time step t (Fig. 2).

With Δt considered to be 100 ms, a sampling time step of 20 ms is selected for the RBF WASP. In other words the problem is formulated as a multiple step ahead prediction using neural networks. Fig. 1 shows the schematic diagram for training the proposed WASP. The two RBF networks receive the same inputs but at different moments in time. The first network is trained using supervised learning to track the plant states at time step $(t-5)$, given the plant states and measurements at time steps $(t-10)$, $(t-15)$ and $(t-20)$.

At each time step the updated output weight matrix and the RBF unit centers of the first network are transferred to the second network, which receives the same type of data at time steps $(t-5)$, $(t-10)$ and $(t-15)$, and predicts the plant states at time step t. The predicted output of the second neural network in Fig. 1 is also improved by adding the previous time step error $E(t-5)$ to it. This is similar to the correct path of a typical Kalman filter [24]. This improves the accuracy of the neuroidentifier prediction.

At first, small and large scale disturbances are applied to the power system in a way that they excite all the modes of the power system. In a real power system, where applying faults to the system is not feasible, this large amount of data can be gathered by sampling the system inputs and outputs over a long period of time. Using the large amount of data samples of the problem space, the RBFN centers are first derived using an offline batch-mode clustering technique [25]. The centers are kept fixed during the operation of the WASP in order to ensure the stability of the RBFN. The plasticity of the RBFN is achieved by continuously updating the output weight matrix using the backpropagation algorithm. This helps the RBFN to respond to minor changes and deviations in the power network.

However, the RBFN should also be robust to the changes in the power system configuration and operating conditions. This is achieved by applying a quasi-online training algorithm for updating the centers: In a window of 50 samples (1 s), the distances of the RBFN centers with the newly arrived data are compared for each center. If, for any of the centers this difference is larger than a user defined tolerance level η, then the center is marked as a *potential* center for updating. At the end of the time window, the five centers that show the worst performance, i.e., largest overall distance with the new data, are updated. The centers are then fixed until the end of the next evaluation. The number of centers to be updated depends on the problem and the performance of the neural network.

2) Missing Sensor Restoration: The missing sensor restoration algorithm in Fig. 2 consists of a neural network based autoencoder (Fig. 3) that is trained to learn the relationship among the sensor outputs throughout the power system. Essentially, it is a multilayer perceptron (MLP) neural network that has fewer neurons in the hidden layer than in the input layer, and is trained offline to learn an identity mapping between its inputs and outputs [26]. The data runs through a bottleneck that reduces the degrees of freedom among the sensor data. Supervised learning is applied for training the autoencoder. Convergence of the weights of the autoencoder means that the input set can be reconstructed from the reduced data set. All the plant states X and the measurements Z along with their two times delayed values are fed into the autoencoder.

In general, the autoencoder learns to perform a projection operation onto a subspace spanned by the training data.

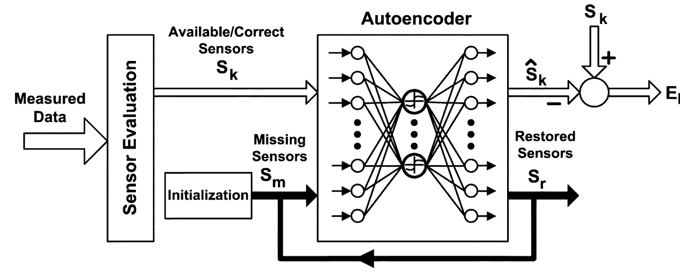

Fig. 3. Missing sensor restoration structure.

Narayanan *et al.* [26] proposed an approach based on projection onto convex sets (POCS) for restoring the missing data. In this technique, the outputs of the autoencoder corresponding to the lost data are iteratively fed back to the autoencoder inputs until the solution converges. In Fig. 3 the output S_{r} of the autoencoder associated with the missing sensors S_{m} is fed back to its input. The portion of the output corresponding to the healthy sensor readings is ignored.

This process is iterated back and forth until a certain stopping criterion is reached. There should be a maximum number of iterations defined for the process to ensure that a final estimate of the outputs of the missing sensors is made available as inputs to the WASP on time. Moreover, the error between the correct sensor readings and their estimates (the output of the autoencoder) should be closely watched, i.e., the signal E_k in Fig. 3. An increase in this error indicates that the iteration process has diverged and the final results should not be used for the neuroidentifier.

More details on the structure and training of the WASP can be found in [27].

V. Wide Area Controller

Fig. 4 shows the schematic diagram of the WAC. It is based on the adaptive critic designs (ACDs) theory that enables the controller to deal with nonlinear nonstationary systems in the presence of noise and uncertainties [28]. This technique has been successfully applied by the authors for designing optimal internal controllers for a STATCOM in a multimachine power system [29], [32]. The controller consists of a Critic neural network, which is trained to estimate the cost-to-go function $J(t)$ in the Bellman's equation [28]. Once its weights have converged, the Critic network is used to train a second network, an Action neural network that provides the auxiliary reference signals $A(t)$ for the three generators' AVRs and the STATCOM voltage reference. The vector V_{ref} in Fig. 4 denotes the vector of steady state voltage set-points for the AVRs of the three generators and the STATCOM line voltage control loop.

An ACD based wide area neurocontroller can serve as a hierarchical controller for the power system. While the primary level of control still comprises of the local controllers of the components in the power network, the Action network performs as a secondary level controller which closes the loop and provides set-point control of the local controllers. The optimization responsibilities of the third level control are accomplished by the Critic network that tries to optimize the system performance by

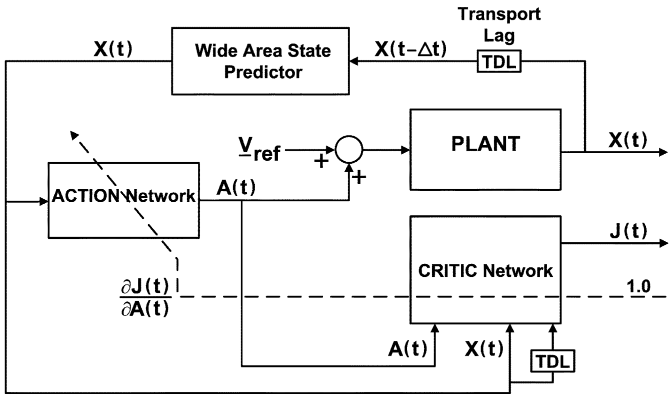

Fig. 4. Schematic diagram of the WAC.

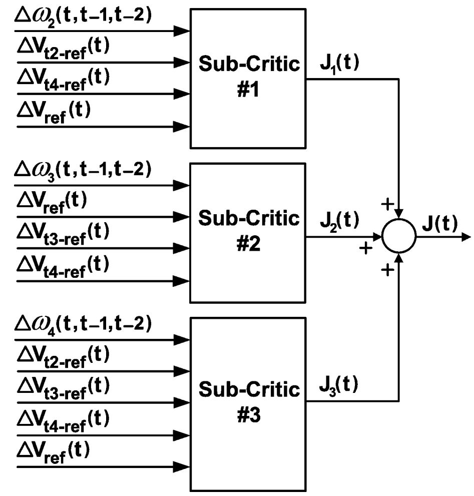

Fig. 5. Schematic diagram of the WAC Critic network.

providing the appropriate training signals for the Action network.

A. Utility Function

The vector of the states of the power system is considered to be comprised of the speed deviations of the three generators (Gen 2, Gen 3 and Gen 4 in Fig. 1) in (1)

$$X(t) = [\Delta\omega_2(t), \Delta\omega_3(t), \Delta\omega_4(t)]^T. \tag{1}$$

A utility function decomposition approach is adopted that helps speed up the training process of the Critic network [31]. Three separate utility function components U_2, U_3 and U_4 are defined for the WAC

$$U(t) = U_2(t) + U_3(t) + U_4(t) \tag{2}$$

where each function U_j corresponds to the speed deviations of one of the synchronous generators, i.e., $\Delta\omega_j$

$$U_j(t) = |\Delta\omega_j(t) + \Delta\omega_j(t-1) + \Delta\omega_j(t-2)|. \tag{3}$$

The utility function decomposition applied here is due to the fact that the rotors of the three generators have different mechanical swings and therefore, the WAC should try to improve the performance of all three at the same time. If all three rotor speeds are considered in one single utility function, then they might at times cancel out each other's effect, which can result in, for example, a low value for the utility function during a large fault. The cost-to-go function estimated by the Critic network is

$$J(t) = \sum_{i=0}^{\infty} \gamma^i \cdot U(t+i) \tag{4}$$

which can be further simplified as

$$J(t) = \sum_{i=0}^{\infty}\left(\sum_{j=2}^{4}\gamma^i.U_j(t+i)\right) = \sum_{j=2}^{4} J_j(t). \tag{5}$$

For the effects of the discount factor γ the reader is referred to [28], [31].

B. Critic Network Structure

Three sub-Critic networks are used in this paper, one for each of the three utility functions U_2, U_3 and U_4 respectively, where each one learns one part of the cost-to-go function. Fig. 5 shows the schematic diagram of the Critic network. It consists of three separate MLP neural networks with 10 neurons heuristically chosen in the hidden layer with hyperbolic tangent as the activation function. Since an action dependent ACD controller design is adopted in this study [28], the controller outputs need to be incorporated into the input vectors of the three sub-Critic networks as well. The ACD neurocontroller in Fig. 4 generates four auxiliary reference signals for the power system

$$A(t) = [\Delta V_{\mathrm{t2-ref}}(t), \Delta V_{\mathrm{t3-ref}}(t), \Delta V_{\mathrm{t4-ref}}(t), \Delta V_{\mathrm{ref}}(t)]^T. \tag{6}$$

For an action dependent Critic network, it is possible to feed all four control outputs in $A(t)$ to each sub-Critic. However, not all the control outputs affect all the state variables in (2). In fact, some of the control outputs have negligible effect on certain state variables. For instance, synchronous generators 2 and 3 are far from one another and therefore, the effect of the auxiliary control signal applied to the AVR of each one on the rotor speed deviations of the other one can be ignored. Simplifying the structures of the sub-Critics by removing the unnecessary control outputs can help speed up the training process of each sub-Critic network. According to the discussion above, the structure of the Critic network is illustrated in Fig. 5.

The three sub-Critics can be trained independently one-by-one, or simultaneously. The details of training the Critic neural networks are provided in the authors' previous work in [29], [30].

C. Action Network

As mentioned in Section I, one of the main objectives of having a wide area control scheme in the power network is to be able to respond to a system disturbance with the least amount of

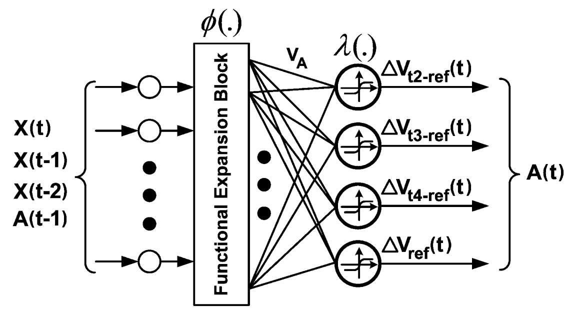

Fig. 6. Schematic diagram of the WAC Action network.

control effort possible. This means that the WAC needs to ensure that undesired interactions between the controllers are reduced. A MLP neural network cannot be an effective choice, due to the fact that in such a network every output error has a direct impact on all the weights of the input weight matrix. This means that in an MLP neural network the outputs interact with one another and the error in each one affects the others (see [27] for details). A WAC Action network designed using MLP networks will therefore create unwanted interactions between the controllers, whereas the idea behind the WAC is to generate an auxiliary reference signal for each local controller based on the effect of only that controller on the cost-to-go function.

This issue can be solved by using a functional link (FNL) neural network. These neural network structures were originally proposed by Pao *et al.* [32]. Using orthogonal mathematical functions $\Phi(\cdot)$, a FNL expands the m-dimensional input space to the M-dimensional hyperspace, where $M \geq m$. These orthogonal functions, which can range from polynomials to trigonometric functions, form the bases for the FNL neural network.

Fig. 6 illustrates the schematic diagram of the FNL Action neural network, where V and $\lambda(\cdot)$ are the output weight matrix and the output activation function respectively. In this structure, the hidden layer is replaced by the Function Expansion block; therefore, the input weight links are removed as well. This prevents the output error of the k^{th} node to affect the signal generated by any of the other output layer neurons and therefore, there is no interaction between the different control signals. Instead, the WAC control signals try to independently control their corresponding local controller based on their individual effect on the overall cost-to-go function defined for the power system.

A Chebyshev based FNL neural network is used in this paper for $\Phi(\cdot)$, where the first four Chebyshev functions are considered to be the activation (basis) functions

$$\begin{aligned}\phi_0(x) &= 1.0, \phi_1(x) = x\\ \phi_2(x) &= 2x^2 - 1, \phi_3(x) = 4x^3 - 3x.\end{aligned} \tag{7}$$

The Action network receives the values of the power system states X at time steps (t), $(t-1)$ and $(t-2)$, along with the Action network outputs at $(t-1)$, and in turn generates the control signal at time (t). The activation functions in (7) are applied to all the entries of the Action network input vector. Therefore, with the inputs to the Action network considered as in Fig. 6, and the basis functions defined in (7), the FNL expands the 13-dimensional input space to a $13 \times 4 = 52$ dimensional hyperspace. The output of the Action network will be added to the AVRs of the three generators and the STATCOM line voltage reference (Fig. 1). The outputs of the Action network are clamped in a way that the terminal voltages of the generators or the voltage at bus 4 in Fig. 1, where the STATCOM is connected to the power system, never go beyond the acceptable range of $[0.95, 1.05]$ p.u.

1) Action Network Pre-Training Stage: Often it is necessary to pre-train the Action network before connecting it to the plant. In the case of supervisory level control, where the neural network is dealing with deviation signals, the Action network control loop can be closed and its output applied to the plant with a randomly initialized set of synaptic weights. The initial weights can be limited to a very small value so that they do not have much impact on the power system in the first stages of the training. As time goes by, the magnitudes of the Action network weights are increased and its outputs start impacting the power system. However, it is also possible to pre-train the Action network, using supervised learning, in order for the weights to converge to values that can help stabilize the power system right from the start. These values are the target signals that are defined by the user and are used in the supervised learning process. The weights after the pre-training stage are used as the starting point of the final training stage where the performance of the neurocontroller is improved towards an optimal nonlinear controller. If the target signals for the pre-training stage are chosen correctly, the above procedure will expedite the overall learning process of the Action network.

A pre-training stage is executed for the WAC in this paper, during which three power system stabilizers are installed on the three generators. The neurocontroller is trained to learn the dynamics of the three PSSs. The first three outputs of the WAC are related to the three generators and the fourth output corresponds to the STATCOM line voltage controller. The latter is forced to follow the output provided by a linear combination of speed deviations of generators 3 and 4 [27]. Therefore, the target signal for the Action network pre-training stage is defined as

$$\begin{aligned}A^*(t) = [&V_{PSS2}(t), V_{PSS3}(t),\\ &V_{PSS4}(t), k(\Delta\omega_3(t) + \Delta\omega_4(t))]^T.\end{aligned} \tag{8}$$

Clearly, the above target vector is far from optimal; however, it provides a starting point solution for the Action network final training stage. Using a supervised learning scheme, the Action network weights are now trained for 500 s in order to follow the target vector defined in (8). The Action network is not controlling the plant at this stage; therefore, its outputs are not applied to the AVRs or the STATCOM.

2) Action Network Final Training Stage: With the Critic network and the Action network weights already converged during the pre-training stages, the ACD neurocontroller is now ready to control the power system. Therefore, the supervisory control loop can be closed by applying the Action network outputs to the voltage references of the AVRs of the three generators and the STATCOM. At this stage, the Critic network is providing the appropriate training signal for the Action network (Fig. 4).

The power system is now exposed to large scale faults and disturbances, such as three phase short circuits along different

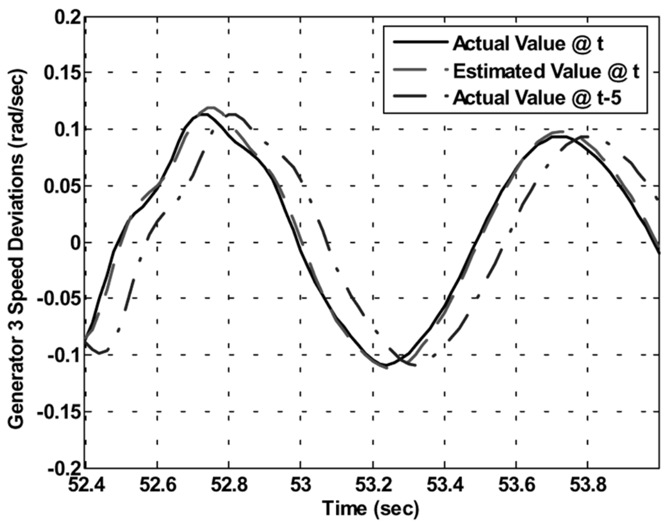

Fig. 7. Actual and estimated speed deviations of generator 3 during case study 1.

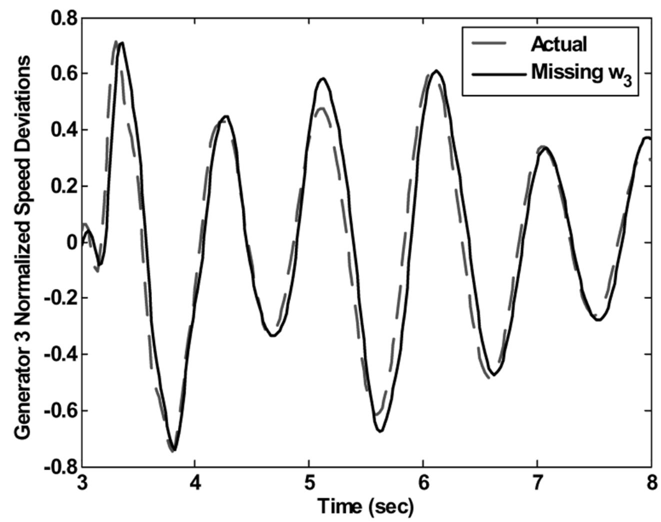

Fig. 8. Actual and estimated speed deviations of generator 3 during case study 2.

transmission lines and buses. The deviations of the generator rotor speeds create a nonzero utility function and therefore, a positive cost-to-go function $J(t)$ estimated by the Critic network. Both the Action and Critic networks undergo training in order to learn the dynamics of the power system during the large natural faults. An annealing learning rate scheme is used for both the Action and Critic. During this process, training starts with a learning rate of about 0.1 for the Critic and 0.01 for the Action, which gradually decreases to a value of 0.005 for the Critic and 0.001 for the Action network. This ensures that during the initial training stages the neural networks adapt themselves to the plant dynamics quickly, but as the learning process continues, they do not have a drastic reaction to any sudden changes in the plant dynamics. In this way the networks do not forget the previously learned information. During the simulations, the same discount factor and learning rate parameter are assumed for all the three sub-Critic networks. However, in general this is not necessary and the three neural networks can undergo training with different parameters. The training process continues at various operating conditions, with different faults and disturbances, until a good accuracy and acceptable performance is achieved by the ACD neurocontroller.

VI. Simulation Results

A. Wide Area State Predictor

1) Case Study 1: Static Transport Lag: In the first test, one of the transmission lines connecting buses 3 and 4 in Fig. 1 is disconnected, thereby changing the configuration of the power system. Fig. 7 shows the speed deviations of generator 3 estimated by the WASP. The value at $(t-5)$ is the delayed information available and transmitted to the WASP. However, the simulation results clearly indicate that the WASP compensates very well for the 100 ms transport lag.

2) Case Study 2: Missing ω_3: In the second test, a 100 ms three phase short circuit occurs after 3 s at the middle of one of the transmission lines connecting buses 3 and 4 during which the sensor that reads the generator 3 speed fails. The missing sensor restoration part in Fig. 2 is therefore activated and using the available healthy data restores the missing information, which is now fed to the neuroidentifiers in order to predict the values of the missing speed deviations in real-time (Fig. 8).

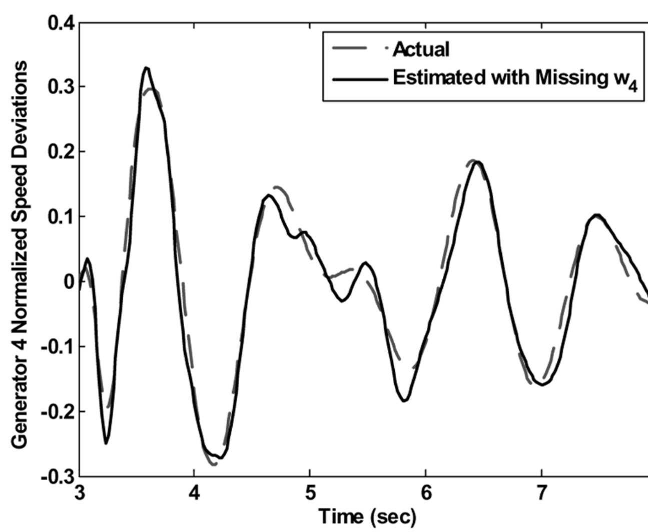

Fig. 9. Actual and estimated speed deviations of generator 4 during case study 3.

3) Case Study 3: Missing Speed Signal (ω_4): A test similar to case study 2 is carried out now with the sensor of the rotor speed of generator 4 failed during a three phase short circuit applied at the middle of the transmission line connecting buses 2 and 5. Fig. 9 illustrates the response of the WASP that is able to restore the missing speed sensor information using the autoencoder to a reasonable degree of accuracy.

B. Wide Area Controller

Several tests are now carried out in order to compare the effectiveness of the proposed WAC with locally tuned PSSs as well as an uncompensated power system with no PSSs. The parameters and the structure of the power system stabilizers is given in Appendix B.

1) Case Study 4: A Three Phase Short Circuit at Bus 5: In the first of these tests, a three phase short circuit occurs at bus 5.

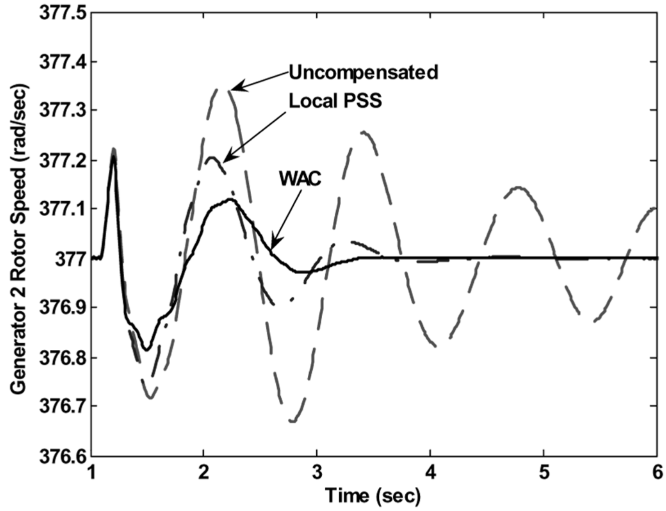

Fig. 10. Rotor speed deviations of generator 2 during case study 4.

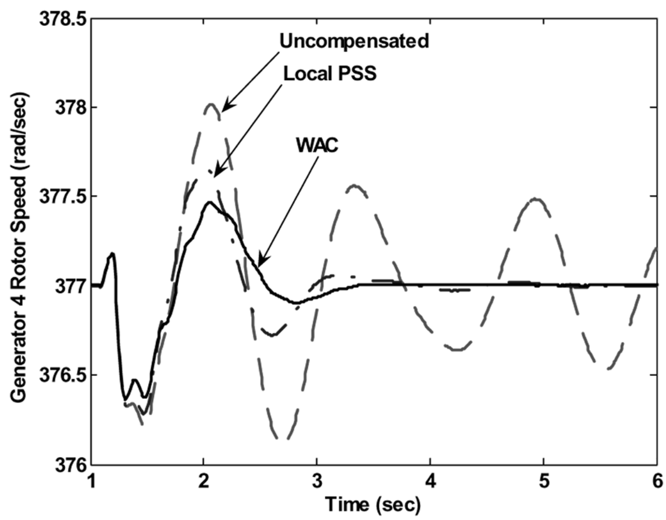

Fig. 11. Rotor speed deviations of generator 4 during case study 5.

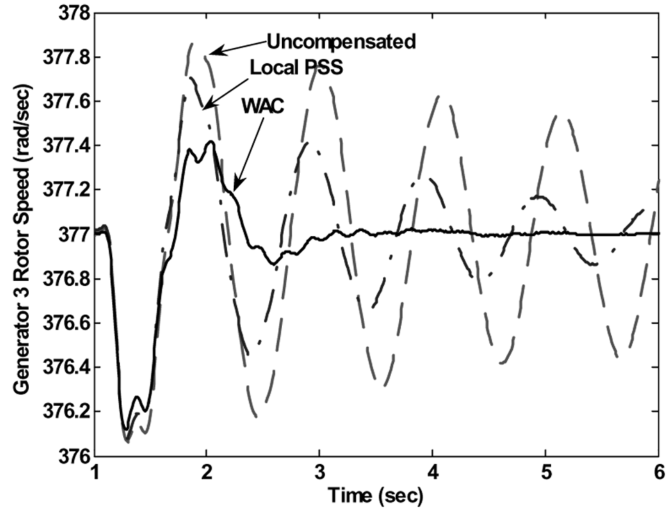

Fig. 12. Rotor speed deviations of generator 3 during case study 6.

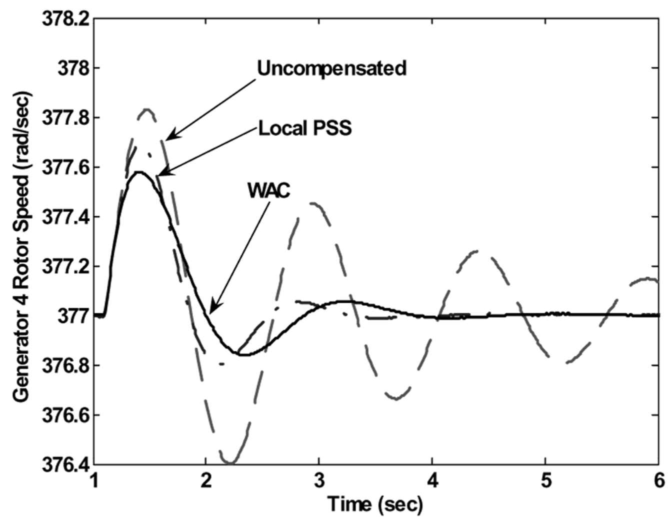

Fig. 13. Rotor speed deviations of generator 4 during case study 6.

The fault is cleared after 100 ms and therefore, it does not permanently change the power system topology. Fig. 10 illustrates some typical results and shows that the WAC is only slightly more effective than the local PSS in damping out the speed oscillations.

2) Case Study 5: A Three Phase Short Circuit at the Middle of the Transmission Line 3–4: In the next test, a 100 ms three phase short circuit is applied at the middle of one of the parallel transmission lines connecting buses 3 and 4. The line is disconnected after the fault is cleared. Fig. 11 compares the performances of the WAC and the local PSSs with an uncompensated system and shows that the WAC is more effective than the case of the power system compensated with local PSSs.

3) Case Study 6: Transmission Line 4–6 Disconnected: The next test investigates the effect of a major change to the topology of the power system by switching off a transmission line which connects buses 4 and 6. This changes the operating condition of the power system and therefore reduces the efficiency of the locally tuned stabilizers that are normally tuned to provide effective damping in a certain frequency range. Figs. 12–13 contain some typical results. Fig. 13 shows that for generator 4 the local PSS is still performing effectively; however, the WAC is considerably more effective for rotor speed deviations in generator 3 (Fig. 12). This can be due to the fact that the dynamics of generator 3 are affected more by the topology change in the power system.

Fig. 14 illustrates the signal applied to the terminal voltage reference of generator 3 during the disturbance; the signal exerted by the WAC is of the same magnitude but it is generated in an intelligent way that helps the controller damp out the oscillations faster.

4) Case Study 7: Three Phase Short Circuit at the Middle of the Transmission Line 2–5: The transmission line 4–6 of the previous case study is reconnected to the power system. A three phase short circuit now occurs at the middle of the line connecting buses 2 and 5. The fault is cleared after 100 ms, but the line remains disconnected. Figs. 15 and 16 show the rotor speed deviations of generators 3 and 4. Since the operating conditions and the topology of the power system change as a result of the fault, the performances of the local PSSs are slightly degraded. However, the WAC manages to restore the system to the steady state conditions in less time.

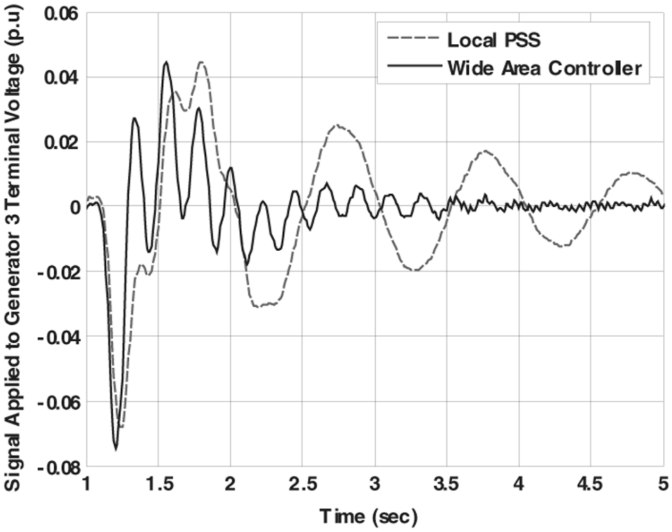

Fig. 14. Signal applied to the voltage reference of generator 3 during case study 6.

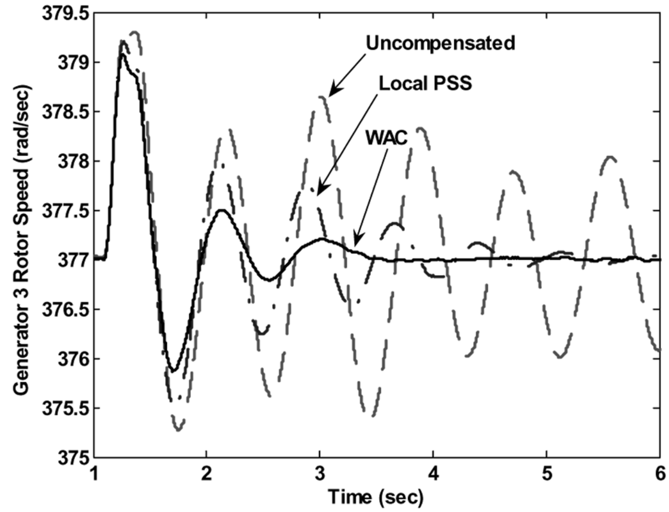

Fig. 17. Rotor speed deviations of generator 3 during case study 7.

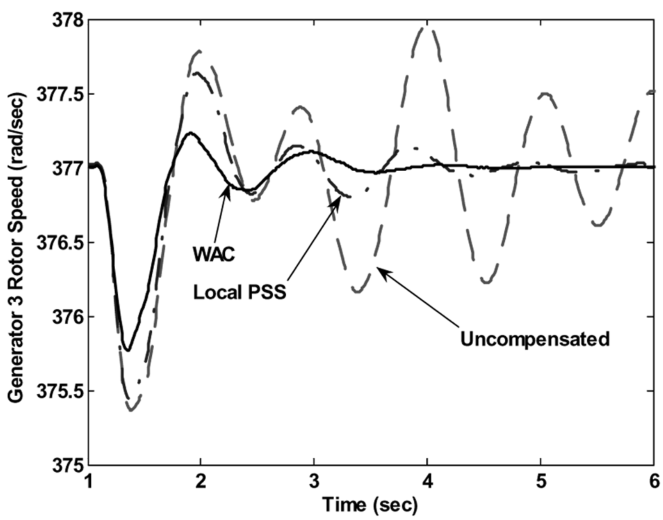

Fig. 15. Rotor speed deviations of generator 3 during case study 7.

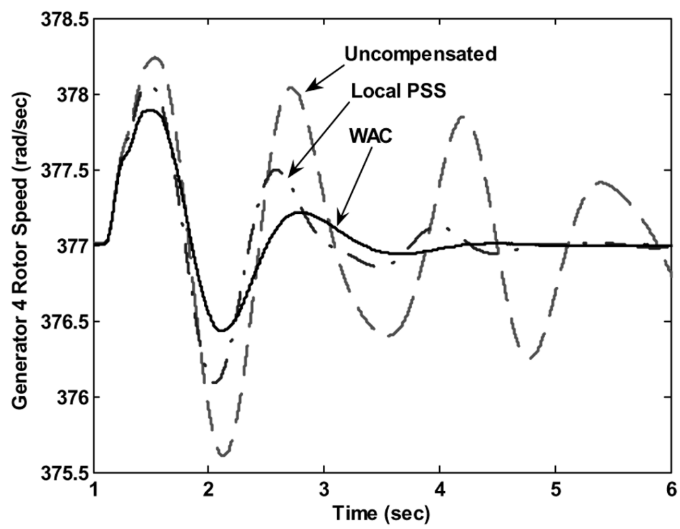

Fig. 18. Rotor speed deviations of generator 4 during case study 7.

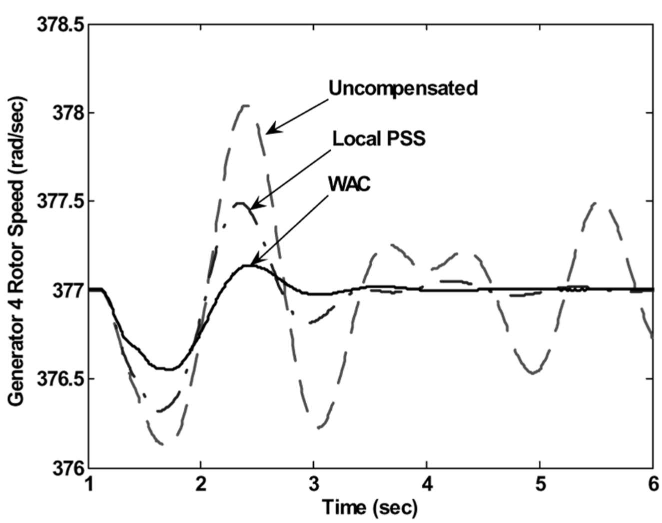

Fig. 16. Rotor speed deviations of generator 4 during case study 7.

5) Case Study 8: Load Disconnected: In the next test, the operating condition of the power system is changed by changing the active power reference of generators 3 and 4. After the power system reaches the new steady state point, the shunt load in bus 4 is disconnected and the results are shown in Figs. 17–18. The local PSS for generator 2 still manages to damp out the oscillations almost as fast as the WAC; however, the performances of the local stabilizers on generators 3 and 4 are noticeably degraded. Also, Fig. 19 depicts the control signal applied to the terminal voltage reference of generator 4.

6) Stability Analysis: In order to compare the efficiency of the proposed WAC and the local power system stabilizers in providing overall stability for the power system, three phase short circuits are separately applied to the terminals of the three generators and the critical clearing time is compared for the cases where the power system is being controlled by three local PSSs as well as the case where the proposed WAC is controlling the power system. The results indicate that the two control schemes provide the same critical clearing time during large scale short circuits applied to the power system. Fig. 20 shows some typical results which correspond to a 340 ms three phase short circuit at the terminals of generator 3 in Fig. 1. Both controllers follow the

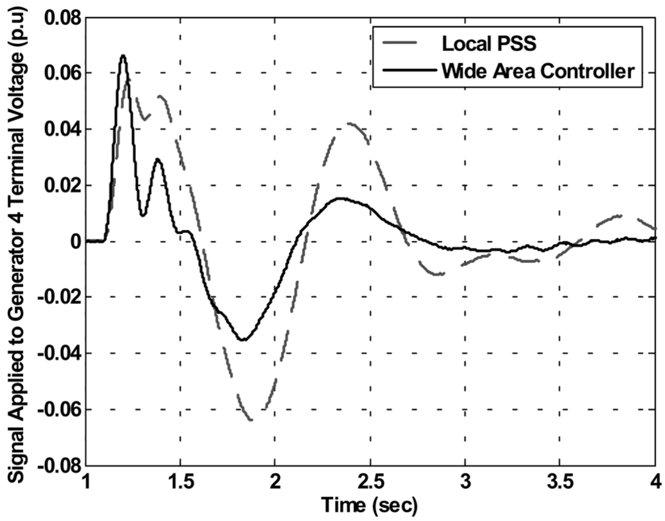

Fig. 19. Signal applied to the terminal voltage reference of generator 4.

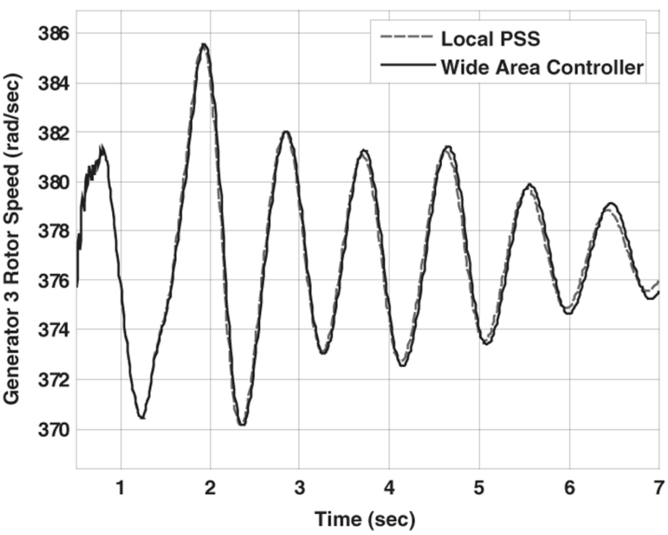

Fig. 20. Generator 4 rotor speed during a 340 ms three phase short circuit at the terminals of the generator.

same trajectory of speed, due to the fact that the control signals are being limited by the hard limiters at the output of the PSSs and the WAC. For any longer clearing time, none of the controllers are able to restore the system to steady state conditions.

7) Performance Measurement: In this section, the damping performance in the power system with the WAC, with the local PSSs and with no compensation is compared. A performance index $(P \cdot I_i)$ in (9) is defined to measure the damping

$$P \cdot I_i = \left(\sqrt{\frac{1}{N}\sum_{k=1}^{N}\Delta\omega_{2,k}^2} + \sqrt{\frac{1}{N}\sum_{k=1}^{N}\Delta\omega_{3,k}^2} + \sqrt{\frac{1}{N}\sum_{k=1}^{N}\Delta\omega_{4,k}^2} \right)^{-1} \quad (9)$$

where $\Delta\omega_{j,k}$ represents the k^{th} sample of the rotor speed deviations of the j^{th} generator and index i represents the i^{th} test. A larger value for the performance index indicates a better

TABLE I

PERFORMANCE INDEXES OF THE POWER SYSTEM COMPENSATED BY ACD WAC, THE LOCAL PSSS AND THE UNCOMPENSATED SYSTEM

TYPE OF TEST	NO WIDE AREA CONTROL	LOCAL PSSS FOR GENERATORS	ACD WIDE AREA CONTROLLER
Short circuit at bus 5	1.33	3.55	4.15
Short circuit along the transmission line 3-4	1.17	2.28	2.94
Transmission line 4-6 switch on/off	1.26	2.49	3.20
Short circuit along the transmission line 2-5	0.93	1.78	2.41
Load disconnected	0.71	1.27	1.59
Overall performance index	0.204	0.404	0.516
Normalized overall performance index	1.0	1.98	2.52

damping during the large scale disturbances applied to the power system. During each fault/disturbance applied to the system, 100 samples are taken at 0.1-s intervals from each rotor speed in 10 s of simulation. The performance indexes of different controllers are evaluated during various faults and the final performance index is derived according to (10)

$$P \cdot I = \left(\sum_i \frac{1}{P \cdot I_i} \right)^{-1}. \quad (10)$$

The overall performance index of each control scheme summarized in Table I is defined as in (10). In the last row of the Table I the overall performance indexes are normalized based on the overall performance index of the uncompensated system, to show that during large scale disturbances the proposed neural network based WAC improves the performance of the power system by about 150% and 30% compared to the power system with no wide area control and the power system with individual local PSSs on the generators, respectively.

VII. PRACTICAL CONSIDERATIONS

A. Hardware Implementation

The proposed ACD based wide area controller and the state predictor can be efficiently implemented on a DSP board. Venayagamoorthy *et al.* [33], [34] have reported successful implementation of a neurocontroller for a turbogenerator. Also, Venayagamoorthy and Ray [16] have shown that an ACD based power system stabilizer can be implemented on a DSP board. The controller, built on a DSP board, sends the control signals to the power system which is implemented on a Real-Time Digital Simulator (RTDS).

B. Real-Time Development of the WAC

For real-time development of the WAC, the pre-training stages can be executed offline using the data points obtained from the power system during its normal performance as well as disturbances. Also, the final training stage can be conducted online as the WAC is controlling the plant.

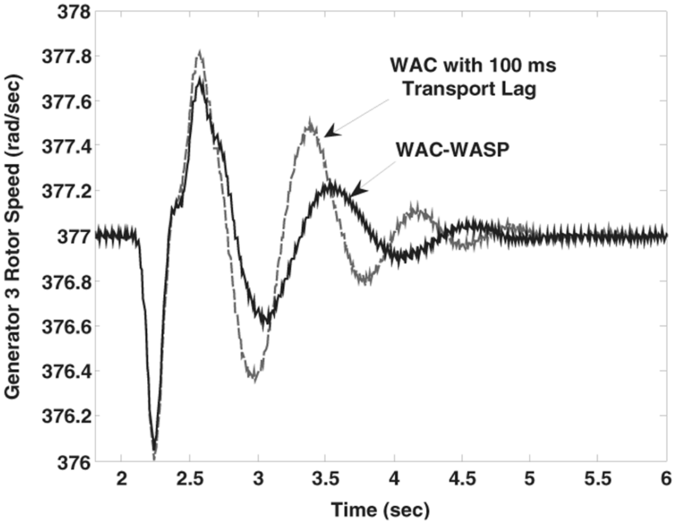

Fig. 21. Generator 3 rotor speed during a 100 ms three phase short circuit at the transmission line 4–6.

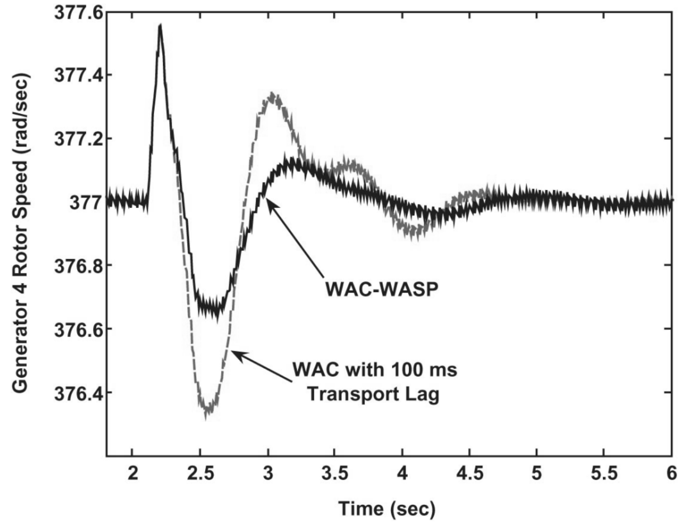

Fig. 22. Generator 4 rotor speed during a 100 ms three phase short circuit at the transmission line 4–6.

If the data set is sufficiently large, the WAC weights are fixed after convergence and remain constant thereafter. Otherwise, a quasi-online approach can be adopted which allows adjusting the weights of the two neural networks during the operation of the WAC. In this case, during a certain sampling window whose length is predefined by the design engineer, data points are obtained from the power system and a batch mode backpropagation [25] is applied to adjust the weights of a neural network identical to the Critic network. After the weights of this shadow-Critic converge, they are downloaded to the actual Critic network. This will ensure stability of the WAC. A similar approach can also be adopted for the Action network.

C. *Selecting the Proper Control Signal*

Throughout this study the authors have considered the rotor speed of the generators as the measured signal for the WAC and have assumed that the signal is available at the terminals of the generator and can be transmitted to the WAC (except for the cases that it is being predicted by the WASP). In most cases, this is a valid assumption. The local power system stabilizers are often designed based on the generator speed signal as well.

However, it should be noted that other available signals such as the active power can be used for designing the WAC as well. This is due to the fact that as long as a reasonable relationship exists between the measured signals and the control signals, a Critic network with converged weights can provide the correct training signals for the Action network. In such case, it might be helpful to introduce more measured signals as the system states in order to enable the Action network to learn the relationship between the power system inputs and outputs more effectively.

VIII. Conclusions

A neural network based optimal wide area controller (WAC) design is presented in this paper for hierarchical control of a 12-bus benchmark power system together with a STATCOM. Based on the speed deviations on the three generators in the power system, the WAC generates auxiliary control signals in the form of voltage references for the voltage references of the AVRs of the three generators and of the STATCOM, in order to improve the dynamic stability of the power system during large scale disturbances.

Using adaptive critic designs theory, the WAC is able to provide nonlinear optimal control over the infinite horizon of the problem, with no need to any mathematical model of the power system or the STATCOM. Reinforcement learning is applied for training the external controller, which makes it largely insensitive to the size of the power system. Simulation results show that the proposed WAC is more effective than locally tuned PSSs for the three generators for damping the speed deviations of the generators neighboring the STATCOM.

Also, a radial basis function network (RBFN) based wide area state predictor has been presented in this paper that estimates the plant states based on the available measurements with delays. Moreover, by using a neural network based autoencoder, the proposed WASP is able to restore the missing data from the available data in case of having failed sensors or longer than expected transport lags. Several case studies have been carried out to validate that the WASP is able to estimate the plant states in real-time with good accuracy at various operating conditions and system contingencies. Such a scheme can be effectively used in any wide area or supervisory level controller in a power system.

Appendix

Effect of Transport Lag Compensation: The effect of the transport lag compensation is evaluated in this section. A 100 ms three phase short circuit is applied to the power system at the middle of the transmission line connecting buses 4 and 6. The line is restored after the fault is cleared. Figs. 21 and 22 illustrate the rotor speed deviations of generators 3 and 4 controlled by the WAC for two cases: one with a transport lag of 100 ms and the other with the WASP to predict the real-time value. The results clearly indicate that the existence of the WASP for compensating the transport lag helps the dynamic performance of the power system.

Parameters of the Local PSS: The structure of the local power system stabilizers used in this study is illustrated in Fig. 23. It consists of a proportional gain, lead compensators

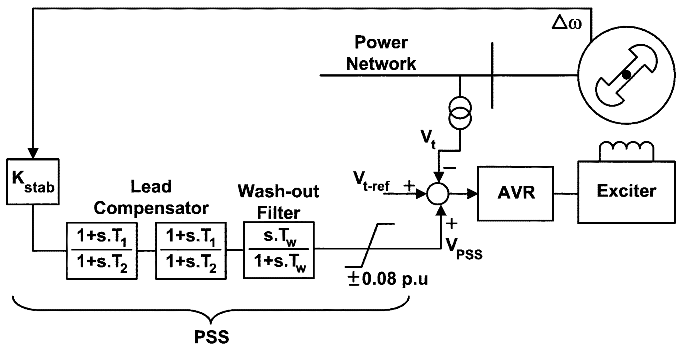

Fig. 23. Structure of the local power system stabilizers.

TABLE II
PARAMETERS OF THE LOCAL POWER SYSTEM STABILIZERS.

GENERATOR	K_{STAB}	T_1	T_2
Gen 2	8	0.2	0.05
Gen 3	12	0.29	0.06
Gen 4	10	0.28	0.05

and a wash-out filter with a time constant of 10 s. The filter is used to prevent the PSS from responding to slow dynamic changes in the rotor speed that are normally responded to by the governor.

Table II summarizes the parameters of the three power system stabilizers.

REFERENCES

[1] P. Kundur, *Power System Stability and Control*. New York: McGraw-Hill, 1994.

[2] N. G. Hingorani and L. Gyugyi, *Understanding FACTS- Concepts and Technology of Flexible AC Transmission Systems*. New York: IEEE Press, 1999.

[3] T. S. Yoo and S. Lafortune, “Decentralized supervisory control with conditional decisions: Supervisor existence,” *IEEE Trans. Automat. Contr.*, vol. 49, no. 11, pp. 1886–1904, Nov. 2004.

[4] H. Ni, G. T. Heydt, and L. Mili, “Power system stability agents using robust wide area control,” *IEEE Trans. Power Syst.*, vol. 17, no. 4, pp. 1123–1131, Nov. 2002.

[5] H. F. Wang, “Multi-Agent coordination for the secondary voltage control in power system contingencies,” *Proc. Inst. Elect. Eng.*, vol. 148, no. 1, pp. 61–66, Jan. 2001.

[6] D. Karlsson, M. Hemmingsson, and S. Lindahl, “Wide area system monitoring and control,” *IEEE Power Energy Mag.*, pp. 68–76, Sep. –Oct. 2004.

[7] S. A. Arafeh, “Hierarchical control of power distribution systems,” *IEEE Trans. Automat. Contr.*, vol. AC-23, no. 2, pp. 333–343, Apr. 1978.

[8] A. Rubaai and F. E. Villaseca, “Transient stability hierarchical control in multimachine power systems,” *IEEE Trans. Power Syst.*, vol. 4, no. 4, pp. 1438–1444, Oct. 1989.

[9] F. A. Okou, L. A. Dessaint, and O. Akhrif, “Large power system stability enhancement using wide-area signals based hierarchical controller,” in *Proc. IEEE PES 2004*, Jun. 2004, vol. 2, pp. 1583–1589.

[10] J. Posser, J. Selinsky, H. Kwanty, and M. Kaml, “Supervisory control of electric power transmission networks,” *IEEE Trans. Power Syst.*, vol. 10, no. 2, pp. 1104–1110, May 1995.

[11] C. W. Taylor, D. C. Erickson, K. E. Martin, R. E. Wilson, and V. Venkatasubramanian, “WACS- wide area stability and voltage control system: R&d and online demonstration,” *Proc. IEEE*, vol. 93, pp. 892–906, May 2005.

[12] M. E. Aboul-Ela, A. A. Sallam, J. D. McCalley, and A. A. Fouad, “Damping controller desing for power system oscillations using global signals,” *IEEE Trans. Power Syst.*, vol. 11, no. 2, pp. 767–773, May 1996.

[13] J. H. Chow, J. J. Sanchez-Gasca, H. Ren, and S. Wang, “Power system damping controller design using multiple input signals,” *IEEE Contr. Syst. Mag.*, pp. 82–90, Aug. 2000.

[14] I. Kamwa, R. Grondin, and Y. Hébert, “Wide-Area measurement based stabilizing control of large power systems- a decentralized/hierarchical approach,” *IEEE Trans. Power Syst.*, vol. 16, no. 1, pp. 136–153, Feb. 2001.

[15] B. Chaudhuri, R. Majumder, and B. C. Pal, “Wide-Area measurement based stabilizing control of power system considering signal transmission delay,” *IEEE Trans. Power Syst.*, vol. 19, no. 4, pp. 1971–1979, Nov. 2004.

[16] G. K. Venayagamoorthy and S. Ray, “A neural network based optimal wide area control scheme for a power system,” in *Proc. IEEE IAS*, Hong Kong, Oct. 2005, vol. 1, pp. 700–706.

[17] G. W. Kim and K. Y. Lee, “Coordination control of ULTC transformer and STATCOM based on an artificial neural network,” *IEEE Trans. Power Syst.*, vol. 20, no. 2, pp. 580–586, May 2005.

[18] C. W. Taylor, D. C. Erickson, K. E. Martin, R. E. Wilson, and V. Venkatasubramanian, “WACS- wide-area stability and voltage control system: R&D and online demonstration,” *Proc. IEEE*, vol. 93, pp. 892–906, May 2005.

[19] S. Jiang, U. D. Annakkage, and A. M. Gole, “A platform for validation of FACTS models,” *IEEE Trans. Power Delivery*, vol. 21, pp. 484–491, Jan. 2006.

[20] G. K. Venayagamoorthy, Y. d. Valle, S. Mohagheghi, W. Qiao, S. Ray, R. G. Harley, D. M. Falcao, G. N. Taranto, and T. M. L. Assis, “Effects of a STATCOM, a SCRC and a UPFC on the dynamic behavior of a 45 bus brazilian power system,” in *Proc. IEEE PES Inaugural Conf. Expo.*, Durban, South Africa, Jul. 11–15, 2005, pp. 305–312.

[21] C. W. Taylor, M. V. Venkatasubramanian, and Y. Chen, “Wide area stability and voltage control,” in *Proc. Symp. Specialists in Electric Operational and Expansion Planning*, Curitiba, Brazil, May 2000.

[22] M. A. El-Sharkawi and R. J. Marks, II, “Missing data restoration for system control and diagnostics,” in *Proc. Symp. Diagnostics for Electric Machines, Power Electronics and Drives*, Atlanta, GA, Aug. 2003, pp. 338–341.

[23] A. Monticelli, “Electric power state estimation,” *Proc. IEEE*, vol. 88, no. 2, pp. 262–281, Feb. 2000.

[24] G. Welch and G. Bishop, An Introduction to the Kalman Filter Univ. North Carolina at Chapel Hill, 2004, Tech. Rep..

[25] S. S. Haykin, *Neural Networks: A Comprehensive Foundation*, 2 ed. Englewood Cliffs, NJ: Prentice-Hall, 1998.

[26] S. Narayanan, R. J. Markds, II, J. L. Vian, M. A. El-Sharkawi, and B. B. Thompson, “Set constraint discovery: Missing sensor data restoration using auto-assocoative regression machines,” in *Proc. Int. Joint Conf. Neural Networks (IJCNN)*, May 2002, vol. 3, pp. 2872–2877.

[27] S. Mohagheghi, “Adaptive Critic Designs Based Neurocontrollers for Local and Wide Area Control of a Multimachine Power System With a Static Compensator,” Ph.D. dissertation, School of Electrical and Computer Engineering, Georgia Institute of Technology, Atlanta, 2006.

[28] P. J. Werbos, “New directions in ACDs: Keys to intelligent control and understanding the brain,” *Proc. IEEE-INNS-ENNS*, vol. 3, pp. 61–66, Jul. 2000.

[29] S. Mohagheghi, Y. d. Valle, G. K. Venayagamoorthy, and R. G. Harley, “A proportional-integrator type adaptive critic designs based neurocontroller for a static compensator in a multimachine power system,” *IEEE Trans. Ind. Electron.*, vol. 54, no. 1, Feb. 2007.

[30] S. Mohagheghi, G. K. Venayagamoorthy, and R. G. Harley, “Adaptive critic designs based neuro-fuzzy controller for a static compensator in a multimachine power system,” *IEEE Trans. Power Syst.*, vol. 21, no. 4, pp. 1744–1754, Nov. 2006.

[31] G. L. Lendaris and J. C. Neidhoefer, “Guidance in the use of adaptive critics for control,” in *Handbook of Learning and Approximate Dynamic Programming*. Piscataway, NJ: IEEE Press, 2004, ch. 4, pp. 97–124.

[32] Y. H. Pao, S. M. Phillips, and D. J. Sobajic, “Neural-Net computing and intelligent control systems,” *Int. J. Contr.*, vol. 56, no. 2, pp. 263–289, 1992.

[33] G. K. Venayagamoorthy, R. G. Harley, and D. C. Wunsch, II, “Implementation of adaptive critic based neurocontrollers for turbogenerators in a multimachine power system,” *IEEE Trans. Neural Networks*, vol. 14, no. 5, pp. 1047–1064, Sep. 2003.

[34] G. K. Venayagamoorthy and R. G. Harley, “A continually online trained neurocontroller for excitation and turbine control of a turbogenerator,” *IEEE Trans. Energy Conversion*, vol. 16, pp. 261–269, Sep. 2001.

Salman Mohagheghi (S'99) was born in Manchester, U.K., in 1976. He received the B.Eng. degree from the University of Tehran, Iran, in 1999 and the M.Sc. degree from Sharif University of Technology, Tehran, in 2001, both in power electrical engineering. In 2006, he received the Ph.D. degree in electrical engineering from the Georgia Institute of Technology, Atlanta.

He is currently doing research as a Postdoctoral Fellow at the Georgia Institute of Technology. His research focuses on wide area control in power systems, protective relaying, and distributed state estimation.

Dr. Mohagheghi is a member of the IEEE Neural Network Society. He was also the Vice-President of the IEEE PES Student Chapter at the Georgia Institute of Technology from 2003 to 2005.

Ganesh K. Venayagamoorthy (S'91–M'97–SM'02) received the B.Eng. (Hon.) degree with first class honors in electrical and electronics engineering from Abubakar Tafawa Balewa University, Bauchi, Nigeria, and the M.Sc.Eng. and Ph.D. degrees in electrical engineering from the University of Natal, Durban, South Africa, in March 1994, April 1999, and February 2002, respectively.

He was a Senior Lecturer at the Durban Institute of Technology prior to joining the University of Missouri-Rolla (UMR) in May 2002. He is currently an Associate Professor of electrical and computer and the Director of the Real-Time Power and Intelligent Systems Laboratory at UMR. His research interests are in power systems stability and control, computational intelligence, alternatives sources of energy and evolvable hardware. He has published about 200 papers in refereed journals and international conference proceedings.

Dr. Venayagamoorthy is a recipient of the following awards: a 2004 NSF CAREER Award, the 2006 IEEE Power Engineering Society Walter Fee Outstanding Young Engineer Award, the 2006 IEEE St. Louis Section Outstanding Section Member Award, the 2005 IEEE Industry Applications Society (IAS) Outstanding Young Member Award, the 2005 South African Institute of Electrical Engineers (SAIEE) Young Achievers Award, the 2004 IEEE St. Louis Section Outstanding Young Engineer Award, the 2003 International Neural Network Society (INNS) Young Investigator Award, a 2001 IEEE Computational Intelligence Society (CIS) Walter Karplus Summer Research Award and five prize papers with the IEEE Industry IAS and IEEE CIS. He is also a recipient of the 2006 UMR School of Engineering Teaching Excellence Award and the 2005 UMR Faculty Excellence Award. He is an Associate Editor of the IEEE TRANSACTIONS ON NEURAL NETWORKS. He is a Senior Member of the SAIEE, a Member of INNS, the Institute of Engineering & Technology, UK, and the American Society for Engineering Education (ASEE). He is currently the IEEE St. Louis CIS and IAS Chapter Chairs, the Chair of the Task Force on Intelligent Control Systems and the Secretary of the Intelligent Systems subcommittee of IEEE Power Engineering Society and the Chair of the IEEE CIS Task Force on Power System Applications. He is listed in the 2007 edition of *Who's Who in America*.

Ronald G. Harley (M'77–SM'86–F'92) received the M.Sc.Eng. degree (cum laude) in electrical engineering from the University of Pretoria, South Africa, in 1965, and the Ph.D. degree from London University, London, U.K., in 1969.

In 1971, he was appointed to the Chair of Electrical Machines and Power Systems at the University of Natal, Durban, South Africa. At the University of Natal, he was a Professor of electrical engineering for many years, including time as the Department Head and Deputy Dean of Engineering. He is currently the Duke Power Company Distinguished Professor at the Georgia Institute of Technology, Atlanta. His research interests include the dynamic behavior and condition monitoring of electric machines, motor drives, power systems and their components, and controlling them by the use of power electronics and intelligent control algorithms. He has co-authored some 380 papers in refereed journals and international conferences and three patents.

Dr. Harley is a Fellow of the British IEE. Ten of his papers have won prizes from journals and conferences. He is also a Fellow of the Royal Society in South Africa and a Founder Member of the Academy of Science in South Africa formed in 1994. During 2000 and 2001, he was one of the IEEE Industry Applications Society's six Distinguished Lecturers. He was the Vice-President of Operations of the IEEE Power Electronics Society (2003–2004) and Chair of the Atlanta Chapter of the IEEE Power Engineering Society. He is currently Chair of the Distinguished Lecturers and Regional Speakers program of the IEEE Industry Applications Society. He received the Cyrill Veinott Award in 2005 from the Power Engineering Society for "Outstanding contributions to the field of electromechanical energy conversion."